ISSN: 2319-5967
ISO 9001:2008 Certified
International Journal of Engineering Science and Innovative Technology (IJESIT)
Volume 2, Issue 5, September 2013

Piezoelectric Energy Harvesting with Frequency Tuning for Ventilation System Monitoring

Joseph R. Davidson and Changki Mo
Washington State University Tri-Cities, School of Mechanical and Materials Engineering
2710 Crimson Way, Richland, WA. U.S.A.

Abstract*— This paper describes the modeling and testing of a piezoelectric energy harvester designed to convert ambient vibrations generated by an industrial facility's ventilation fans into the electric energy required to sustain a wireless industrial health monitoring system providing feedback about the ventilation system's performance. Experimental results show that a cantilever energy harvester with a fundamental frequency matching the input frequency of the exhaust fan produces useful electric power. However, the excitation frequency is not constant and as it diverges from the fundamental frequency of the harvester system performance rapidly deteriorates. Therefore, a harvester with a tunable fundamental frequency is needed in order to provide useful energy across a range of excitation frequencies. Previous studies have shown that tuning of an operating energy harvester can be accomplished with the use of magnets. For this study the fundamental frequency of the cantilever is tuned by varying the distance between two magnets. Results show that system performance is improved by tuning the frequency of the harvester to match a spectrum of excitation frequencies.

Index Terms— **Energy Harvesting, Frequency Tuning, Piezoelectric, Ventilation System Failure Monitoring.**

I. INTRODUCTION

In 2011 an operating industrial facility at Hanford, WA experienced a catastrophic failure of one of its electric centrifugal exhaust fans. A follow up investigation into the cause of the incident determined multiple potential failure modes, including impeller failure, failure of the inner bearing pillow block mounting bolts, and over-heating and failure of the outer bearing [1]. Further evaluation of the system's other six fans revealed some cracks on impeller blades typical of metal fatigue due to dynamic loads. There is a high probability that axial vibration was a contributing cause to the fan failure. Even though four of the exhaust fans have far exceeded their original design life, it may be more feasible and a better use of resources to extend the life of the fans rather than replace them outright as the facility is scheduled for demolition in the next several years. Continuous feedback about the fans' operating performance would be useful in extending the equipment's life and continuing to support their safety function. An autonomous structural health monitoring system (SHM) could provide instant notification of excessive vibration levels that could threaten personnel and potentially damage equipment.

Rapid advances in wireless technologies and low-power electronics have enabled the increased use of autonomous systems for the monitoring of structural health. The use of wireless structural health monitoring systems presents several advantages, one of the most significant being that wireless systems can provide continuous monitoring without the associated installation costs of wiring, which, depending upon the size of the sensor network can be prohibitively expensive [2]. Because many wireless sensor nodes are powered by traditional batteries that must inevitably be replaced, recent research has focused on developing systems that can be powered by harvesting ambient energy, such as mechanical vibrations, sunlight, and wind, directly from their environments. This paper evaluates the feasibility of using a piezoelectric device to harvest energy from a ventilation system's vibrations in order to power a wireless SHM system.

The industrial ventilation system mentioned previously serves as a case study that guides the design considerations and modeling parameters of the piezoelectric energy harvester presented in this paper. Most importantly, because the vibration frequencies change due to varying plant ventilation requirements, harvesters that can provide useful electric energy across a range of frequencies are required. Therefore, nonlinear energy harvesters with frequency tuning are considered. After presenting an analytical model for calculating the power output of a piezoelectric cantilever beam, an empirical model for tuning the fundamental frequency of the beam with magnets is reviewed. A piezoelectric energy harvester is then fabricated and tested in order to compare the analytical and experimental results. Finally, the power output of a harvester with the capacity for frequency tuning is compared with the power output of a standard, linear resonant harvester.

ISSN: 2319-5967
ISO 9001:2008 Certified
International Journal of Engineering Science and Innovative Technology (IJESIT)
Volume 2, Issue 5, September 2013

II. PIEZOELECTRIC ENERGY HARVESTING

The general theory behind kinetic energy harvesting is to use a transduction mechanism to generate electric energy from motion. Over the past decade most attention has focused on the use of the piezoelectric transduction mechanism to convert vibration to electric energy. The piezoelectric effect was discovered in 1880 when J. and P. Curie found that certain crystals subjected to mechanical strain became electrically polarized and that the degree of polarization was proportional to the applied strain [2]. When a piezoelectric material is placed under a mechanical stress, an open circuit voltage appears across the material, and when a voltage is applied to the material, a mechanical stress develops in the material [3]. Piezoelectric materials are usually anisotropic, so the properties of the material differ depending upon the direction of forces and orientation of the electrodes. The constitutive equations for piezoelectric materials are [3]

$$\delta = \frac{\sigma}{Y} + dE \tag{1}$$

$$D = \varepsilon E + d\sigma \tag{2}$$

where δ is the mechanical strain, σ the mechanical stress, Y the Young's modulus of elasticity, D the electrical displacement (i.e. charge density), E the electric field, ε the dielectric constant, and d is the piezoelectric strain coefficient. These equations describe the mechanical and electrical behavior of the piezoelectric material. Fig. 1 illustrates the operational mode of the piezoelectric harvester designed for this study. The x, y, and z axes are labeled 1, 2, and 3. The harvester is operated in the 31 mode, meaning that stress is induced along the 1 direction and charge is collected on the surface of the 3 direction. Operation in the 31 mode is inherent during bending when large strains develop in the 1 direction. The piezoelectric material can also be used in the 33 mode where forces are applied along the z axis. The advantage of operating in the 31 mode is that larger strains can be produced with smaller input forces, and the fundamental frequency of the system is much smaller [3].

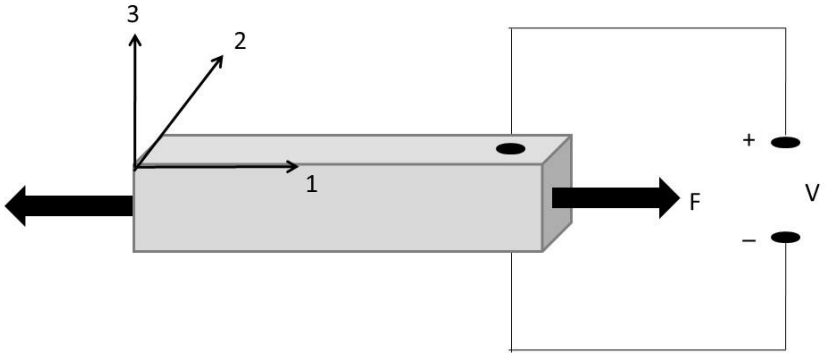

Fig 1: Illustration of the 31 Mode of Operation for a Piezoelectric Cantilever Beam [3].

Many different designs of piezoelectric energy harvesters have been developed. Two common geometries for harvesting energy from vibrations are a unimorph, a cantilever beam with one piezoelectric layer on top of the beam, and a bimorph, which has piezoelectric layers on both the top and bottom of the beam [4]. A cantilever beam has low resonant frequencies that can be further reduced by adding a proof mass on the end of the beam and provides high levels of strain in the piezoelectric layers.

III. NONLINEAR ENERGY HARVESTING

A limitation of linear, resonant piezoelectric energy harvesters is their narrow operating bandwidth [5]. Maximum power is obtained when the fundamental frequency of the harvester matches the excitation frequency. As shown in Chen et al. analysis of a cantilever bimorph [6], the induced voltage drops precipitously for small differences between the excitation frequency and natural frequency of the energy harvester. Frequency matching can be difficult because of manufacturing tolerances, excitation frequency changes, and electric load changes [7]. Recent research has focused on developing broadband energy harvesters that can accommodate variable input frequencies and still provide useful energy [8]-[12]. Two of the tuning methods investigated are the application of axial loads and the use of magnets, both of which change the harvester's stiffness. Cottone et al. [13] modeled and tested a buckled beam under axial compression that exhibited superior power generation compared to the unbuckled beam. Al Ashtari et al. [7] used magnets to design and test an energy harvester with a tunable resonance frequency. Their design is adopted for this study because the tuning technique is relatively simple to set

ISSN: 2319-5967
ISO 9001:2008 Certified
International Journal of Engineering Science and Innovative Technology (IJESIT)
Volume 2, Issue 5, September 2013

up and enables the natural frequency of the harvester to be adjusted during operation.

IV. ANALYTICAL ESTIMATE OF POWER OUTPUT

This section provides the analytical model for estimating the power output of a unimorph cantilever beam. After deriving the analytical model for power output empirical relations are then presented for estimating the tuned natural frequency of the beam as a function of the separation distance between two magnets.

A. *Beam Deflection*

The unimorph composite energy harvester will be modeled as a distributed-parameter system with multiple degrees of freedom using Euler-Bernoulli beam assumptions. The cantilevered beam is under harmonic, steady-state base excitation (Fig. 2).

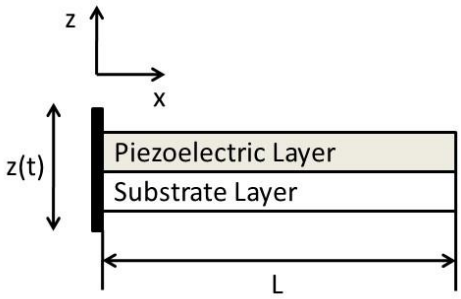

Fig 2: Unimorph Cantilever Beam.

The governing equation of motion for the beam is [14]

$$\frac{\partial^2 w(x,t)}{\partial t^2} + c^2 \frac{\partial^4 w(x,t)}{\partial x^4} = -\frac{\partial^2 z(t)}{\partial t^2}, \quad c = \sqrt{\frac{EI}{\rho A}} \tag{3}$$

where w is the deflection of the beam, ρ is the beam's density, A is the cross-sectional area, E is the Young's modulus of elasticity, I is the cross sectional area moment of inertia about the neutral axis, and z is the base displacement of the beam.

The free vibration equation (3) is a partial differential equation that contains four spatial derivatives and two temporal derivatives. Assuming a general solution to (3) of the form

$$w(x,t) = \sum_{n=1}^{\infty} F_n(x) G_n(t) \tag{4}$$

and using the separation of variables technique, the general mode shape for the beam is found to be [15]

$$F_n(x) = -\alpha_n(\sinh(\beta_n x) - \sin(\beta_n x)) + \cosh(\beta_n x) - \cos(\beta_n x) \tag{5}$$

where

$$\alpha_n = \frac{\sinh(\beta_n L) - \sin(\beta_n L)}{\cosh(\beta_n L) + \cos(\beta_n L)}, \qquad \text{and } \beta_n^4 = \frac{\omega_n^2}{c^2}$$

ω_n^2 is the natural frequency of the n^{th} mode and is found from the characteristic equation for the spatial equation

$$\cos(\beta_n l)\cosh(\beta_n l) + 1 = 0 \tag{6}$$

As the first mode is the mode of interest, ω_n will refer to the natural frequency of the first mode for the remainder of this paper. Because the base excitation is harmonic, the base acceleration can be expressed in terms of the excitation amplitude z_o and excitation frequency ω as

$$\frac{\partial^2 z}{\partial t^2} = -z_o \omega^2 \cos(\omega t) \tag{7}$$

Substituting (7) into the solution for beam deflection after the separation of variables yields

ISSN: 2319-5967
ISO 9001:2008 Certified
International Journal of Engineering Science and Innovative Technology (IJESIT)
Volume 2, Issue 5, September 2013

$$\sum_{n=1}^{\infty} F_n(x)(\ddot{G}_n(t) + 2\,\zeta\omega_n\dot{G}_n(t) + \omega_n^2 G_n(t)) = -z_o\omega^2\cos(\omega t) \tag{8}$$

Note, in (8) modal damping has been included with the temporal equation after the separation of variables. Modal damping includes a viscous energy dissipation term of the form $2\,\zeta\omega_n\dot{G}_n(t)$ where ζ is the damping ratio [15]. Multiplying (8) by the mode shape $F_n(x)$, integrating over the length, and citing the orthonormal properties [6] yields

$$\ddot{G}_n(t) + 2\,\zeta\omega_n\dot{G}_n(t) + \omega_n^2 G_n(t) = -A(L)z_o\omega^2\cos(\omega t)\,, \qquad A(L) = \frac{\int_0^L F_n(x)\,dx}{\int_0^L F_n^2(x)\,dx} \tag{9}$$

Equation (9) is an ordinary differential equation that when solved will include a transient response $G_h(t)$ and a steady-state response $G_p(t)$ [15]. As the steady-state response is the equation of interest, the particular solution is determined by assuming a solution to (9) of the form

$$G_n(t) = A\cos(\omega t) + B\sin(\omega t) \tag{10}$$

Substituting (10) into (9) and solving for the constants A and B yields [6]

$$G_n(t) = Y(\omega)\cos(\omega t - \varphi) \tag{11}$$

where

$$Y(\omega) = \frac{-A(L)z_o\omega^2}{\sqrt{(\omega_n^2-\omega^2)^2 + (2\zeta\omega_n\omega)^2}} \qquad \text{and } \varphi = \tan^{-1}\left(\frac{2\zeta\omega_n\omega}{\omega_n^2-\omega^2}\right)$$

The eigenfunction for the original partial differential equation (4) has the form $F_n(x)G_n(t) = w(x,t)$. Substituting the general solutions for the temporal equation (11) and the mode shape (5) into the eigenfunction yields the general solution for the beam's deflection

$$w(x,t) = \sum_{n=1}^{\infty} Y(\omega)\cos(\omega t - \varphi) * [\cosh(\beta_n x) - \cos(\beta_n x) - \alpha_n(\sinh(\beta_n x) - \sin(\beta_n x))] \tag{12}$$

B. *Strain-induced Voltage and Maximum Power Output*

The axial strain of the beam will be calculated with the radius of curvature approach proposed by Chen et al. [6]. Longitudinal strains in the PZT layer of the beam are proportional to the curvature κ and vary linearly with the distance from the center of the PZT layer z_P to the neutral axis z_N.

$$\epsilon = -\kappa(z_P - z_N) \tag{13}$$

The neutral surface of the composite beam is found with the equivalent area procedure [14]

$$z_N = \frac{\sum z_i dA_i}{\sum dA_i} \tag{14}$$

Where z_i is the location of the neutral surface of layer i in reference to a common plane and dA_i is the cross sectional area of layer i. Curvature is a function of the applied moment M and the resistance of the beam to bending (i.e. flexural rigidity)

$$\kappa = \frac{M}{EI} = \frac{\partial^2 w(x,t)}{\partial x^2} \tag{15}$$

Equation (15) is the differential equation of the deflection curve [16]. Substituting (15) into the expression for the axial strain of the PZT layer results in the following equation

$$\epsilon_p = -\frac{\partial^2 w(x,t)}{\partial x^2}(z_P - z_N) \tag{16}$$

ISSN: 2319-5967
ISO 9001:2008 Certified
International Journal of Engineering Science and Innovative Technology (IJESIT)
Volume 2, Issue 5, September 2013

By Hooke's Law, the axial stress σ_P on the PZT layer is $\sigma_p = \epsilon_p E_p$ where E_P is the Young's Modulus of Elasticity of the PZT layer. Because the external electric field strength is zero, the constitutive equation for the charge density of the PZT layer reduces to

$$D_3 = -d_{31}\sigma_p \tag{17}$$

The total strain induced charge Q on the PZT can be found by integrating the charge density over the entire length of the beam [6]

$$Q = \int_0^L D_3 w_p \, dx = -d_{31} w_p \, E_p \epsilon_p dx \tag{18}$$

$$= -d_{31} w_p E_p Y(w) cos(wt - \varphi)(\beta_1)^2 (z_p - z_N) \int_0^L \cos h(\beta_n x) + \cos(\beta_n x) - \alpha_n (\sinh(\beta_n x) + \sin(\beta_n x)) dx \tag{19}$$

$$= -d_{31} w_p E_p Y(w) cos(wt - \varphi)(\beta_1)^2 (z_p - z_N) * \left[\frac{\alpha_1 \cos(\beta_1 L) - \alpha_1 \cosh(\beta_1 L) + \sin(\beta_1 L) + \sinh(\beta_1 L)}{\beta_1}\right] \tag{20}$$

Where w_P is the width of the piezoelectric layer of the beam. For excitation with certain frequency, the induced open circuit voltage V_{OC} can be calculated as

$$V_{OC} = \frac{Q}{C_p} \tag{21}$$

Where C_P is the internal electrode capacitance and is found by

$$C_p = \frac{\varepsilon_p w_p L}{t_p} \tag{22}$$

Where ε_P and t_P are the permittivity and thickness, respectively, of the PZT layer [17]. Considering the case that a resistor R is connected directly with the vibrating piezoelectric beam as the load, the output voltage V can be expressed as

$$V = IR = \frac{\partial Q}{\partial t} R = j\omega Q R \tag{23}$$

Combining (22) and (23), the output voltage can then be expressed as [17]

$$V = \frac{j\omega C_p R}{1 + j\omega C_p R} V_{oc} \tag{24}$$

Lin et al. [17] extract lumped circuit models from (24) and show that the vibrating beam can be modeled as a sinusoidal current source in parallel with its internal electrode capacitance (Fig. 3) or as a sinusoidal voltage source in series with its capacitance.

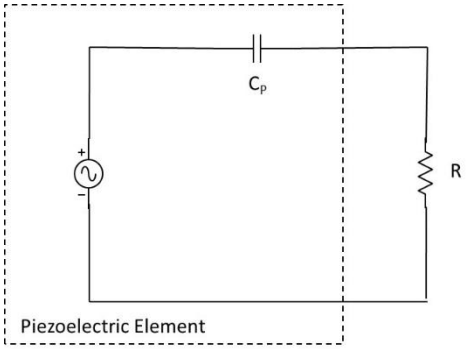

Fig 3: Lumped Circuit Model of Beam as Current Source [17].

The average power on R is [17]

ISSN: 2319-5967
ISO 9001:2008 Certified
International Journal of Engineering Science and Innovative Technology (IJESIT)
Volume 2, Issue 5, September 2013

$$P = \frac{|V|^2}{2R} = \frac{1}{2}\frac{\omega^2 C_p^2 |V_{OC}|^2 R}{1 + (\omega C_p R)^2} \tag{25}$$

The different parameters of the lumped circuit model (i.e. voltage, current, and capacitance) are dependent on the properties of the piezoelectric beam and the vibration source and are independent of the resistive load *R*. So, the generated power can be maximized by optimizing the resistive load. The optimal resistive load and corresponding average output power are found to be [17]

$$R_{opt} = \frac{1}{\omega C_p} \tag{26}$$

$$P_{max} = \frac{\omega C_p |V_{OC}|^2}{4} \tag{27}$$

C. *Magnetic Tuning of the Harvester Frequency*

Tuning of the energy harvester relies upon an empirical magnetic model developed by Ashtari et al**.** [7]**.** A small magnet is added as a tip mass to the free end of a cantilever beam. A second magnet, opposing the first one in the axial direction, exerts an additional force on the vibrating beam that depends on the distance separating the two magnets. The distance between the two magnets *d* can be adjusted without touching the beam so that the harvester can be tuned while in operation. Fig. 4 is a schematic of the experimental set up that will be used for tuning the energy harvester with magnets.

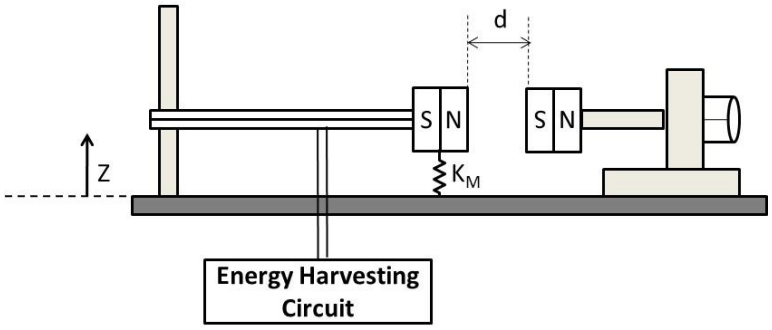

Fig 4: Schematic of Experimental Set Up for Tuning the Energy Harvester [7].

The fundamental frequency of the harvester depends on its effective stiffness and mass. As the mass of the harvester is unaffected by varying the distance between the two magnets, tuning of the harvester is accomplished by using magnetic forces to change the structural stiffness of the cantilever beam. Ashtari et al. model the net effect of the magnetic forces on the beam's stiffness as a nonconventional spring K_M added to the system and show that the fundamental angular frequency ω_n for a cantilever beam with a tip mass and an additional stiffness in the transverse direction is [7]

$$\omega_n = \sqrt{\frac{K_b + K_M}{M_{eq}}} \tag{28}$$

Where M_{eq} is the equivalent mass for a cantilever beam loaded at its free end with a tip mass, K_b is the equivalent structural stiffness of the beam, and K_M is the total magnetic stiffness.

V. HARVESTER FABRICATION

Two unimorph lead zirconate titanate (PZT) energy harvesters were fabricated with PZT-5H4E (Piezo Systems, Inc.) and aluminum. The PZT layer was attached to the aluminum substrate with a two-part conductive epoxy (CW2400, CircuitWorks). The dimensions of the PZT and aluminum layers are provided in Table I.

Table I: Dimensions of the Energy Harvesting Beams

	Width (mm)	Length (mm)	Thickness (mm)
PZT layer	10	45	.127
Aluminum layer	10	45	.127

ISSN: 2319-5967
ISO 9001:2008 Certified
International Journal of Engineering Science and Innovative Technology (IJESIT)
Volume 2, Issue 5, September 2013

A neodymium block magnet (Model B641, K&J Magnetics) was then attached with a two-part epoxy resin to the end of one of the two harvesters. After fabrication the total thickness of the beam was measured with a caliper and was determined to be approximately .381mm. Because the thickness of the bonding layer (.127mm) was equal to that of the aluminum substrate and PZT layer, the beam was modeled as a three-part rather than a two-part composite beam during calculation of the beam's moment of inertia and modulus of elasticity, and the neutral axis of the beam z_N was calculated using the equivalent area procedure.

VI. EXPERIMENTAL SETUP AND HARVESTING CIRCUIT

Experiments were conducted with a unimorph harvester and a unimorph harvester with a magnetic tip mass. To test the energy harvesters the cantilever beams were clamped to an electromagnetic shaker. In order to measure charge output lead wires were attached to the beam with a two part conductive epoxy. The test rig included a power supply for the shaker, an accelerometer attached to the shaker, a function generator, and an oscilloscope. Fig. 5 shows a picture of the harvesting circuit and the harvester attached to the electromagnetic shaker.

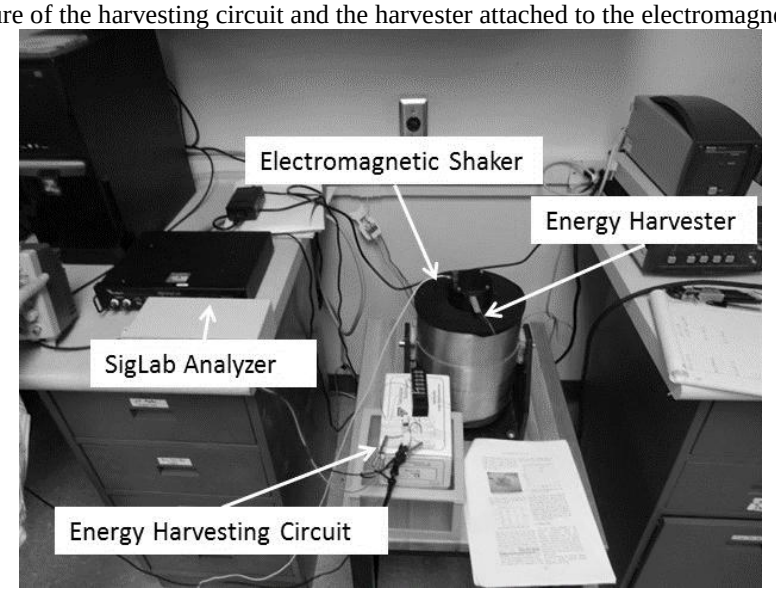

Fig 5: Beam Mounted to the Shaker.

Power was dissipated through a simple resistive load, more specifically, the open circuit voltage rectified through a rectifying bridge and passed into a 10 nF capacitor. Fig. 6 depicts a schematic of the circuit. The voltage across a resistor in parallel with the capacitor was measured.

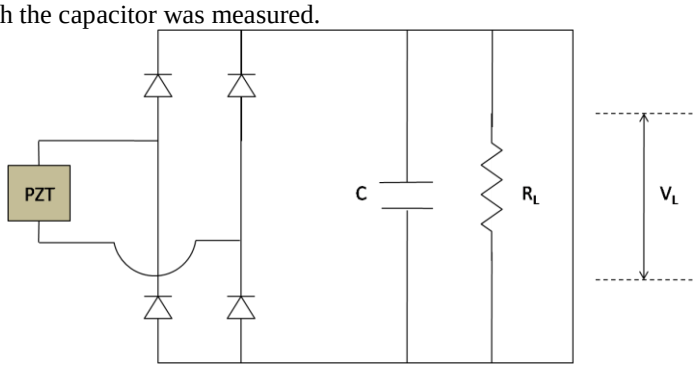

Fig 6: Schematic of the Harvesting Circuit.

In order to tune the harvester with the magnetic tip mass a second magnet was attached to an adjustable slide. The slide was positioned so that the second magnet was at the same height and in-line with the magnet bonded to the free end of the clamped harvester. The distance between the two magnets could be varied while the harvester was in operation by adjusting the position of the slide. Therefore, the voltage across the resistor could be measured as a function of magnet separation distance. Fig. 7 shows a picture of the experimental set-up with the adjustable slide and magnets.

ISSN: 2319-5967
ISO 9001:2008 Certified
International Journal of Engineering Science and Innovative Technology (IJESIT)
Volume 2, Issue 5, September 2013

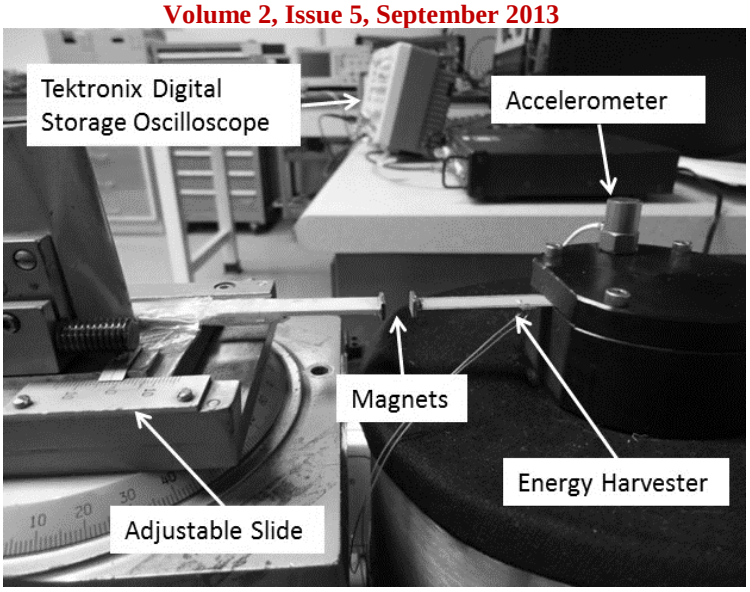

Fig 7: Tuning the Harvester with Magnets.

VII. COMPARISON OF ANALYTICAL MODEL WITH EXPERIMENTAL RESULTS

A. *Simulated and Measured Power Output with Respect to Load (No tip mass)*

During the first experiment the power output versus load resistance was measured for a unimorph energy harvester (without tip mass) for an input vibration equal to the fundamental frequency of the harvester. The characteristics of the excitation force are provided in Table II.

Table II: Properties of Excitation Force (Test 1)

	Acceleration (g)	Amplitude (mm)	Frequency (Hz)	Damping Ratio
Excitation force	.995	.0278	94	.05

Note, the damping ratio ζ was assumed after the experimental results were obtained. By inspection of the data obtained during the experiment it is assumed that a match between the internal PZT impedance and external load impedance occurs at approximately 24 kohm (i.e. the source resistance is 24 kΩ). The simulated power output obtained by the analytical model developed in Section IV is compared with the experimental data in Fig. 8.

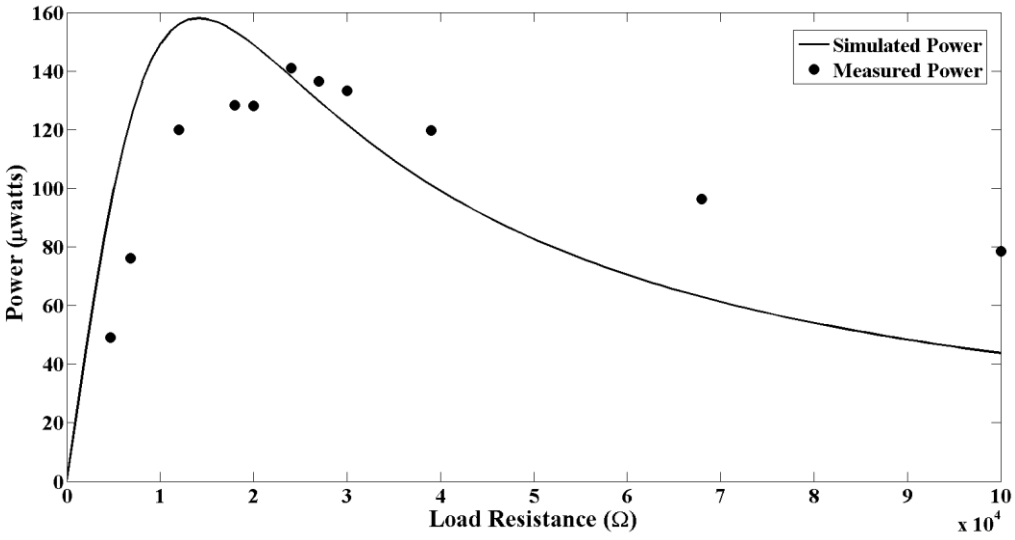

Fig 8: Simulated & Measured Power Output with Respect to Load Resistance (No tip mass).

ISSN: 2319-5967
ISO 9001:2008 Certified
International Journal of Engineering Science and Innovative Technology (IJESIT)
Volume 2, Issue 5, September 2013

The power output obtained during the experiment was approximately 11% less than that predicted by the analytical model. Also, the model predicted smaller source impedance than what was measured.

B. *Simulated and Measured Frequency with Respect to Magnet Separation Distance*

This experiment examined the effect of magnet separation distance on the fundamental frequency of the harvester. Before tuning the beam the load resistance was varied in order to find an impedance match with the source (180 kohm). The load resistance was kept constant at 180 kohm during tuning. As shown in Fig. 7, the slide was adjusted so that the distance between the two magnets varied from 5 mm to 20 mm. The magnets were never brought closer than 5 mm because of the possibility that the magnetic force could fracture the PZT layer of the harvester. At each increment of separation distance the fundamental frequency of the harvester was measured with a dynamic signal analyzer. The experimental results are compared with the simulated frequencies in Fig. 9.

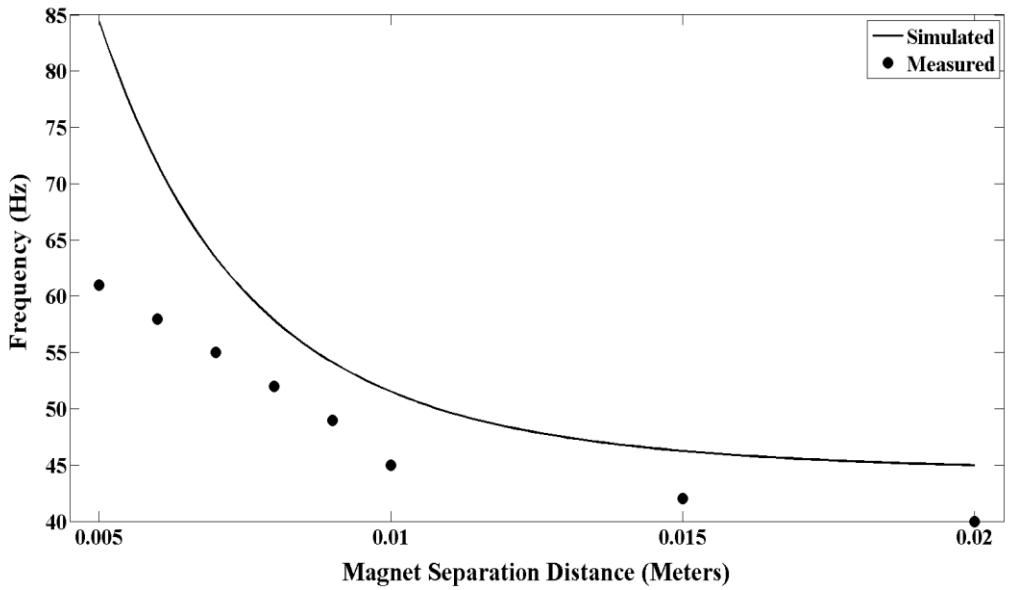

Fig 9: Frequency vs. Magnet Separation Distance

Experimental results show that as the magnets get closer the structural stiffness and fundamental frequency of the harvester increase. Note, the discrepancy between the simulation and measurement results increases when the magnet separation distance reaches approximately 5 mm, at which point the analytical model predicts that the fundamental frequency will rapidly increase. It is apparent from the data that an attractive magnetic force is capable of increasing the fundamental frequency of the energy harvester by increasing its structural stiffness.

C. *Tuned vs. Untuned Power Output*

Fig. 10 compares the tuned and untuned power output of the energy harvester with respect to frequency. For all measurements the load resistance remained constant at 180 kohm. The untuned data points represent the power output of the harvester as the input frequency of the excitation force is adjusted away from the harvester's fundamental frequency of 39 Hz. The data show that, as expected, variations in the excitation frequency cause significant deterioration in system performance. To obtain the tuned data points the excitation frequency was also increased above 39 HZ. Then at each respective input frequency the harvester's fundamental frequency was tuned to match the input by adjusting the separation distance between the vibrating harvester and the second magnet attached to the slide. Power output for the tuned harvester was significantly greater than that of the untuned harvester. For instance, at an excitation frequency of 42 Hz the tuned harvester generated 53 μW compared to the $4.45 \times 10^{-9} W$ produced by the untuned harvester. However, as the difference between the input frequency and the untuned harvester's fundamental frequency (39 Hz) increased the performance of the tuned system deteriorated? This is most likely due to the fact that the impedance of the system changes as its structural stiffness is adjusted with magnetic forces. Load resistances would need to be changed at each magnet separation distance in order to find an impedance match with the load and source.

ISSN: 2319-5967
ISO 9001:2008 Certified
International Journal of Engineering Science and Innovative Technology (IJESIT)
Volume 2, Issue 5, September 2013

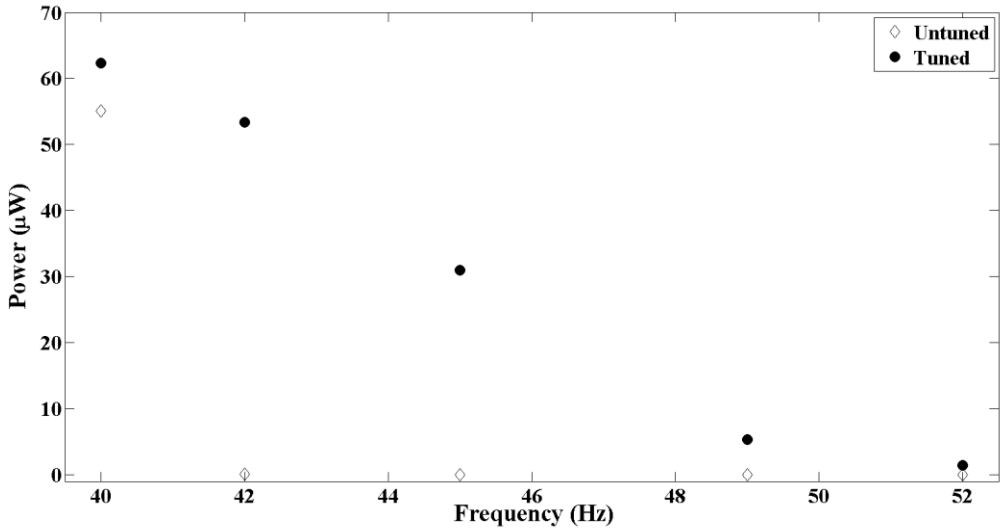

Fig 10: Tuned vs. Untuned Power Output with Respect to Frequency

VIII. CONCLUSION

A tunable PZT energy harvester with a magnetic tip mass was designed and fabricated in order to study the feasibility of using the harvester to convert the frequency-varying ambient vibrations of a ventilation system to the electric energy required to sustain a wireless structural health monitoring network. Simulation and experimental results show that a magnetic attractive force can be used to tune the frequency of the harvester to larger values by increasing its structural stiffness. During this study the harvester's fundamental frequency was tuned to a value 33% greater (52 Hz) than its untuned fundamental frequency (39 Hz). The use of a repulsive magnetic force to reduce the harvester's stiffness thereby lowering its fundamental frequency was not experimentally tested. The power output of the tuned harvester was significantly greater than the output of the untuned beam. Depending on the input frequency, the values for the power generated by the tuned harvester tested during this study were less than 70 μW. Additional parametric study for the optimal harvester than the design tested here may be required in order to provide sufficient energy. Power requirements will also depend on the scheduled operation of the wireless SHM system (i.e. continuous or intermittent usage). Also, a deployed system would have to address impedance matching between the source and load over the range of the excitation frequencies. The experimental results indicate that for a constant load resistance and increasing input frequency the power output of the tuned beam decreases as it becomes stiffer because the impedance match between the harvester and load is lost. An operating system would require an adjustable load resistance in order to provide impedance matching with the energy harvesters across the range of potential tuned frequencies.

REFERENCES

[1] R.D. Gustavson, Exhaust Fan EF-1-25A Failure Evaluation with Recommendations, Hanford, WA: CH2M Hill Plateau Remediation Company (CHPRC), 2011.

[2] S.P. Beeby, M.J. Tudor, and N.M. White, "Energy Harvesting Vibration Sources for Microsystems Applications," Measurement Science and Technology, vol. 17, pp. 175-195, 2006.

[3] S. Roundy, P. Wright, and J. Rabaey, "A Study of Low Level Vibrations as a Power Source for Wireless Sensor Nodes," Computer Communications, vol. 26, pp. 1131-1144, 2003.

[4] A. Khaligh, P. Zeng, and C. Zheng, "Kinetic Energy Harvesting Using Piezoelectric and Electromagnetic Technologies - State of the Art," IEEE Transactions on Industrial Electronics, vol. 57, no. 3, pp. 850-860, 2010.

[5] B. Koser and H. Marinkovic, "Demonstration of Wide Bandwidth Energy Harvesting from Vibrations," Smart Materials and Structures, vol. 21, 065006, 2012.

[6] S.N. Chen, G.J. Wang, and C. Ming-Chun, "Analytical Modeling of Piezoelectric Vibration-Induced Micro Power Generator," Mechatronics, vol. 16, pp. 379-387, 2006.

ISSN: 2319-5967
ISO 9001:2008 Certified
International Journal of Engineering Science and Innovative Technology (IJESIT)
Volume 2, Issue 5, September 2013

[7] W. Al-Ashtari, M. Hunstig, T. Hemsel, and W. Sextro, "Frequency Tuning of Piezoelectric Energy Harvesters by Magnetic Force," Smart Materials and Structures, vol. 21, 035019, 2012.

[8] A. Erturk, J. Hoffmann, and D.J. Inman, "A Piezomagnetic structure for broadband vibration energy harvesting," Applied Physics Letters, vol. 94, 254102, 2009.

[9] S.C. Stanton, C.C. McGehee, and B.P. Mann, "Reversible hysteresis for broadband magnetopiezoelastic energy harvesting," Applied Physics Letters, vol. 95, 174103, 2009.

[10] A.M. Wickenheiser, "Design Optimization of Linear and Non-Linear Cantilevered Energy Harvesters for Broadband Vibrations," Journal of Intelligent Material Systems and Structures, vol. 22, pp. 1213-1225, July 2011.

[11] B.P. Mann and N.D. Sims, "Energy harvesting from the nonlinear oscillations of magnetic levitation," Journal of Sound and Vibration, vol. 319, pp. 515-530, 2009.

[12] A. Erturk and D.J. Inman, "Broadband piezoelectric power generation on high-energy orbits of the bistable Duffing oscillator with electromagnetic coupling," Journal of Sound and Vibration, Vol. 330, pp. 2339-2353, 2011.

[13] F. Cottone, L. Gammaitoni, L., H. Vocca, M. Ferrari, and V. Ferrari, "Piezoelectric Buckled Beams for Random Vibration Energy Harvesting," Smart Materials and Structures, vol. 21, 035021, 2012.

[14] C. Mo, G. Ban, D. Charnegie, and W.W. Clark, "Energy Harvesting from a Vibrating Piezoelectric Unimorph Bender." J. Korean Society of Industrial Application, vol. 10, no. 3, pp. 157-163, 2007.

[15] D.J. Inman, Engineering Vibration, Second Edition, Upper Saddle River, New Jersey: Prentice Hall, 2001.

[16] S.P. Timoshenko and J.M. Gere, Mechanics of Materials, Fourth Edition, Boston: PWS Publishing Company, 1997.

[17] J.H. Lin, X.M. Wu, T.L. Ren, and L.T. Liu, "Modeling and Simulation of Piezoelectric MEMS Energy Harvesting Device," Integrated Ferroelectrics, vol. 95, pp. 128-141, 2007.

[18] W.W. Clark, J.R. Romeiko, D.C. Charnegie, G. Kusic, and C. Mo, "A Case Study in Energy Harvesting for Powering a Wireless Measurement System," 6th International Workshop on Structural Health Monitoring, Stanford University, September 11-13, 2007.

AUTHOR BIOGRAPHIES

Joseph Davidson received the B.S. degree from the United States Military Academy in 2004 and the M.S. degree in Mechanical Engineering from Washington State University in 2013. He is currently working toward the Ph.D. degree in Mechanical Engineering at Washington State University Tri-Cities. His research interests include energy harvesting and dynamics/controls.

Dr. Changki Mo is Assistant Professor in the School of Mechanical and Materials Engineering at Washington State University Tri-Cities. He received his Ph.D. degree in Mechanical Engineering from the University of Oklahoma in 1996. Before joining WSU, Dr. Mo was Visiting Professor in the Department of Mechanical Engineering and Materials Science at the University of Pittsburgh, Pittsburgh, PA and Associate Professor in Automotive Engineering Department at Kyungpook National University (Sangju, South Korea). His research interest includes vehicular and structural vibration control, energy harvesting: self-powered medical implants and self-powered structural health monitoring, micro actuators and sensors, adaptive structure technology, and smart structures for sustainable buildings. Much of his current research focuses on morphing systems using shape memory polymer and piezoelectric systems for actuators, resonators, sensors, or energy sources. He has published about 50 peer reviewed journal and conference articles and one book chapter.